CANADIAN JOURNAL OF EXPLORATION GEOPHYSICS
VOL. 33. NOS. 1 & 2 (DECEMBER 1997), P. 21-28

SIDE-SCANNING SEISMIC IMAGING: A PHYSICAL MODELING STUDY

YE ZHENG AND ROBERT R. STEWART*

ABSTRACT

Off-line seismic energy or side-swipe may complicate conventional seismic records and ultimately lead to erroneous interpretation. However, if 3-component (vertical, radial and transverse) seismic data are available, off-line energy may be attenuated to image below the line or enhanced to image off the line (side-scanning). Different arrival angles of energy from below the seismic line and off-line provide an opportunity to differentiate in-line and off-line energies by their polarization directions. Most previous polarization analysis relies on the eigenvalue method of analysing the covariance matrix of the observed data. This is an effective method, but requires considerable computation. We use a similar but faster direct least-squares method. The main procedures for making an off-line picture are: 1) apply conventional processing (statics, NMO, deconvolution, and stacking) to both vertical and transverse components, 2) apply the polarization filter to the vertical and transverse stacked sections, 3) migrate the stacked section (if necessary), and output the off-line section. We tested this processing flow on physical modeling data. The physical model consists of a plexiglas plate with an embedded "reef". Ultrasonic transducers in vertical and horizontal directions surveyed the "reef" from an offset of 200 m scaled distance. A reasonable off-line image was reconstructed.

INTRODUCTION

In 2-D seismic data, we generally assume that the recorded seismic energy is from directly beneath the seismic line. Data processing procedures (including NMO correction, stack and migration) assume that energy propagates in the vertical plane through the seismic line. Of course, in real seismic data there are reflections and scattered energy from lithologic change or structures away from the line. These off-line energies can degrade the quality of the image from directly beneath the line. For example, if there is a reef beside the seismic line, the line may record both reflections from the interfaces beneath the line and the reef beside the line. On the processed section, there may be a misplaced reef image. To reduce the ambiguity of conventionally processed 2-D seismic sections, we might separate the in-line and off-line energies. We use 3-component seismic data to atempt to: 1) enhance the S/N ratio and improve the quality of the conventionally processed sections by rejecting the off-line energy; 2) build an image of the off-line reflections to get a partial 3-D image from a 2-D seismic line by rejecting in-line enrgy (Zheng and Stewart, 1993; 1994; Zheng, 1995).

Perelberg and Hornbostel (1994) also discussed applications of polarization analysis. One of these applications is the removal of off-line energy. They built a numerical fault and dome model and generated 3-component seismic data. The off-line reflection is removed by a polarization filter using the covariance matrix method. We extend the application of the polarization filter from synthetic data to physical modeling data in this paper and use the filtered data to construct an off-line image.

POLARIZATION FILTERING

Most polarization analysis (e.g., Flinn, 1965; Montalbetti and Kanasewich, 1970; Kanasewich, 1981; Bataille and Chiu, 1991; Perelberg and Horbostel, 1994) is based on the eigenvalue problem of the covariance matrix of seismic data within a time window. The direction of the eigenvector associated with the major eigenvalue is the direction of the major axis of the ellipse of the seismic particle motion. Processing techniques attempt to find a polarization ellipse which best fits the data in the time or frequency domain in a least-squares sense. This is a good method to solve this problem. However, if we try to solve the eigenvalue problem directly, it can be time consuming. The direct least-squares (DLS) method (DiSiena et al., 1984) is another approach to find the direction of the particle motion ellipse and thus the polarization direction of seismic waves.

The DLS method for 2-D data follows (Figure 1). Within a time window, we try to find an axis on which the sum of the squares of the projection is maximum.

$$A(\theta) = \sum_{t=i-L}^{i+L} \left((u_1(t) - x_0)\cos\theta + (u_2(t) - y_0)\sin\theta\right)^2 \quad (1)$$

where, $u_1(t)$ and $u_2(t)$ are the seismic data within a time window. (x_0, y_0) is the geometrical centre of the hodogram (particle motion trajectory).

Veritas Seismic Ltd., 2200, 715 - 5th Avenue SW, Calgary, Alberta T2P 5A2, Tel: (403) 205-6204, e-mail: yeez@vsl.com
* University of Calgary, Calgary, Alberta T2N 1N4, Tel: (403) 220 3265, e mail: stewart@geo.ucalgary.ca

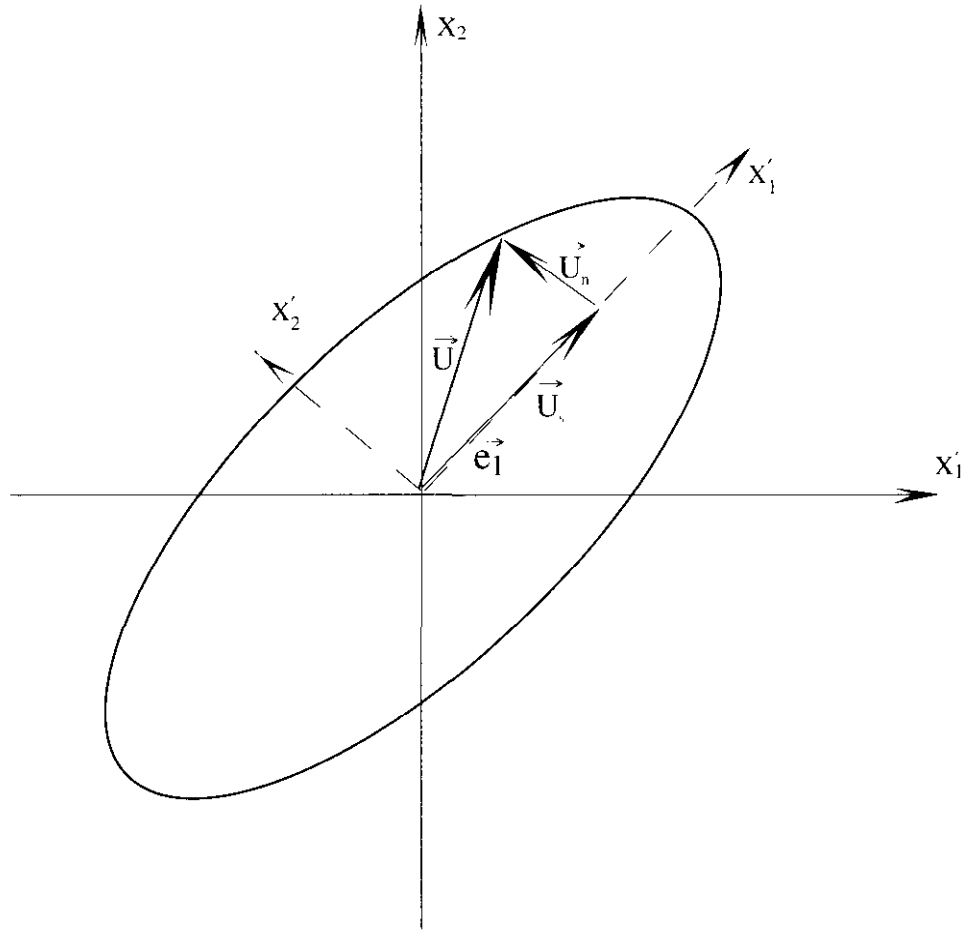

Fig. 1. Schematic diagram of the relationship among the direction of the eigenvector $\vec{e}_1$, trajectory (hodogram) of the particle over the time window $N\Delta t$, and the vector $\vec{U}$ of displacement at the mid-point of the time window. $\vec{U}$ can be divided into two vectors, $\vec{U}_s$ and $\vec{U}_n$. We assume that $\vec{U}_s$ is mainly caused by signal and $\vec{U}_n$ is caused by noise.

After a few mathematical manipulations, we get:

$$\tan 2\theta = \frac{2\psi_{12}}{\psi_{22} - \psi_{11}} \quad , \tag{2}$$

where,

$$\psi_{11} = \sum_{t=j-L}^{j+L} (u_1(t)-x_0)^2 \quad ,$$

$$\psi_{22} = \sum_{t=j-L}^{j+L} (u_2(t)-y_0)^2 \quad ,$$

$$\psi_{12} = \sum_{t=j-L}^{j+L} (u_1(t)-x_0)(u_2(t)-y_0) \quad .$$

After obtaining θ from equation (2), we compare $A(\theta)$ and $A(\theta+\pi/2)$. The direction associated with the larger A is the direction of the major axis of the ellipse, and the smaller correspondents to the minor axis.

We next want to develop a simple filter from the hodogram value. Assuming that $A_1=A(\theta)$ is greater than $A_2=A(\theta+\pi/2)$, we define the first filter factor as:

$$G_1 = 1 - A_2/A_1 \quad . \tag{3}$$

G_1 varies between 0 and 1. For a rectilinear wave, the hodogram should be a line. Therefore the projection of the displacement vector on the line perpendicular to the hodogram line is 0. At this time, G_1 receives its maximum, 1. For a circularly polarized wave, the projection of the displacement vector in any direction is the same. Therefore, A_1 equals A_2. At this time, G_1 is 0.

The direction vector of the major axis of the ellipse is $\vec{e}_1 = (\cos\theta, \sin\theta)^T$, so we can define the second filter factor as follows:

$$G_2' = \left|u(j)\cdot e_1'\right| e_1' = g\,(\cos\theta, \sin\theta)^T \quad , \tag{4}$$

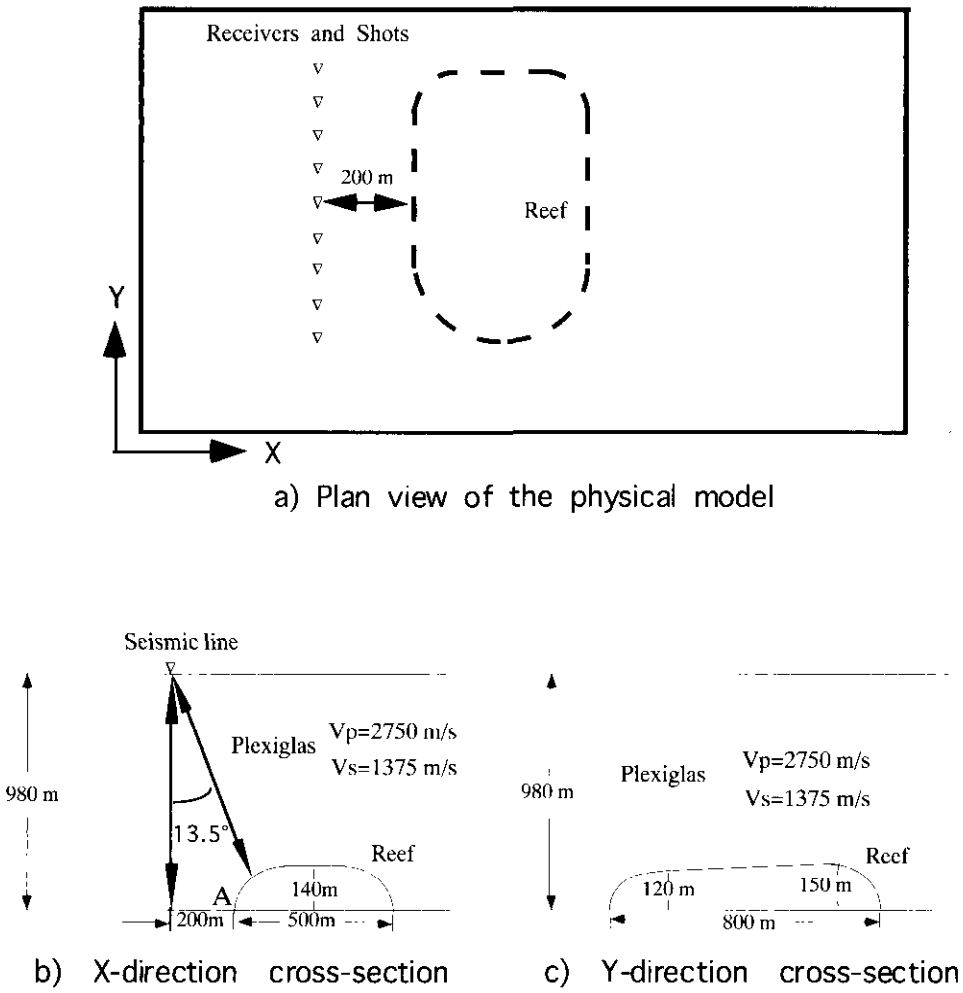

Fig. 2. The physical model used for the side-scanning study.

where, $g = |u_1(j)\cos\theta + u_2(j)\sin\theta|$.

The output of the filter is:

$$\vec{u} = G_1\vec{G_2} = (1\text{-}A_2/A_1)\, g\, (\cos\theta, \sin\theta)^T. \qquad (5)$$

For 3-D data, we can follow similar procedures as with 2-D data. We can project the seismic data to a line and sum up the squares of the projection. The line with the maximum value of the sum of the projection is the major axis of the polarization ellipsoid.

Application to Physical Modeling Data

The physical model we used to test the polarization filter is shown in Figure 2. The physical model under consideration here is made of plexiglas (Figure 3). The "reef" anomaly in the plexiglas plate is simply a milled-out hole. The plate is supported by a jig apparatus (see Figure 4 for the modeling system). The top and bottom surfaces of the layer and the surface of the "reef" are free surfaces. A vertical ultrasonic transducer is used as a source with vertical and horizontal transducers used as receivers. A scale factor between the actual dimension of the model and the field size based on the ultrasonic and seismic frequency is 10,000. The seismic line is then a scaled distance of 200m away from the "reef". The P-wave velocity of the plexiglas is 2750m/s. An end-on spread of receivers is used in this seismic survey. The near offset receiver is 200m and the far offset is 1100m. Both station and shot intervals are 100m giving 10 traces per shot. A total of 12 shots were recorded in the survey. The maximum fold is 5.

A shot record of the physical modeling data is shown in Figure 5. We used the same scale to plot both vertical and transverse components, so the relative amplitude remains unchanged. On both vertical and transverse components, we can see some coherence. The strongest event is at time of about 0.72s for trace 1. It is the reflection from the flat bottom of the model. The signal at time 0.62s for trace 1 is the reflection from the top of the "reef". There is also some coherent noise in the record, consisting of multiples and the reflections from the interfaces between plexiglas layers.

We used conventional techniques to process both vertical

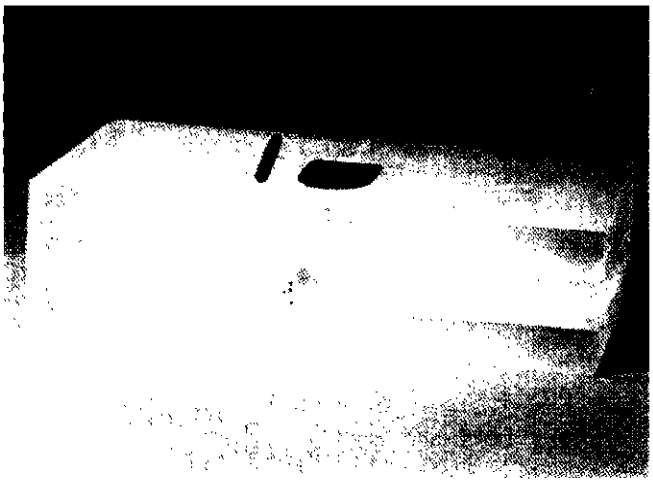

Fig. 3. A photograph of the physical model. We turned the model up side down in order to show the "reef". A pen is placed on the model for scaling.

and transverse components of the physical modeling data. The stacked sections are shown in Figure 6. In both sections, we can see the image of the flat bottom of the model and the "reef". The flat interface is at 0.72s. The "reef" image is in the middle part of the line and at the time of 0.62 s. We also can see clearly the diffraction at the edge of the "reef". There is also an interesting amplitude and the phase change in the flat reflection. In the middle part of the line, the reflection is weaker than that at the ends of the line. The wavelet is changing from zero phase on the ends to mixed phase in the central part. We notice that this anomaly appears at the same location of the "reef" reflection. The lateral distance from point A in Figure 2 to the seismic line is about 200 m. The two-way travel time from point A to the seismic line is about 15ms longer than the two-way travel time from the flat bottom to the line. The dominant frequency of the seismic wave here is about 30 Hz. That means the reflection from point A is delayed about a half cycle compared with the reflection from the flat bottom. Therefore, the energy from the flat bottom is likely decreased by the reflections around point A.

We applied the polarization filter to the physical modeling data. When we use a direction window of 50° - 85°, there is little energy left in the final stacked section (Figure 7). If we use a direction window of 85° - 93°, the "reef" reflection is successfully removed from the stacked section (Figure 8), largely leaving the reflection from the flat bottom of the model. When we change the direction window to 95° - 105°, we remove the reflection from the flat bottom (Figure 9). In this stacked section, there is a clearer picture of the "reef" and other coherent signals are attenuated. When we use the direction window of 105° - 150°, the vertical signals are removed from the stacked section and much of the "reef" energy (Figure 10). We also can calculate the approximate location of the "reef". The two-way travel time of the "reef" reflection measured from Figure 9 is 0.615s. Therefore, the main distance from the imaged part of the "reef" to the seismic line is (refer to Figure 11): $D = 0.615 \times 2750 / 2 = 846$m. The minimum lateral distance from the seismic line is: $S_{min} = D \cos 95° = -74$m. The maximum lateral distance is: $S_{max} = D \cos 105° = -219$m. Similar to the above calculation, the minimum depth of the "reef" is: $D_{min} = D \sin 105° = 817$m. The maximum depth of the "reef" is: $D_{max} = D \sin 95° = 842$m.

These figures are close to the values measured from the model (Figure 2): the distance from the "reef" to the seismic line is 200m and the angle of the raypath from the "reef" is about 103.5°. The actually depth of the "reef" is about 840m.

Polarization Processing Procedures

From three-component seismic data, we can take the vertical and transverse components to enhance the in-line image

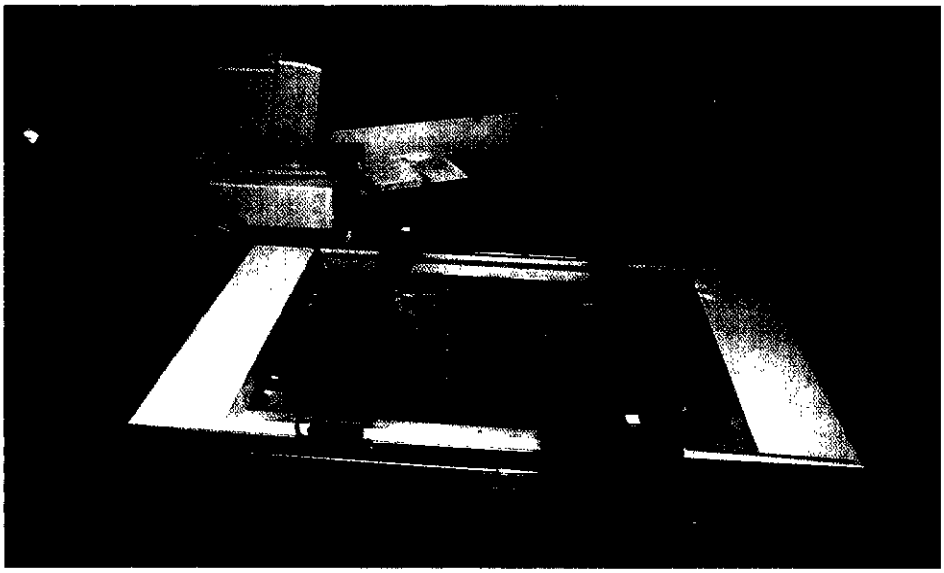

Fig. 4. The ultrasonic physical modeling system. The source (S) and receiver (R) on the plexiglas are indicated.

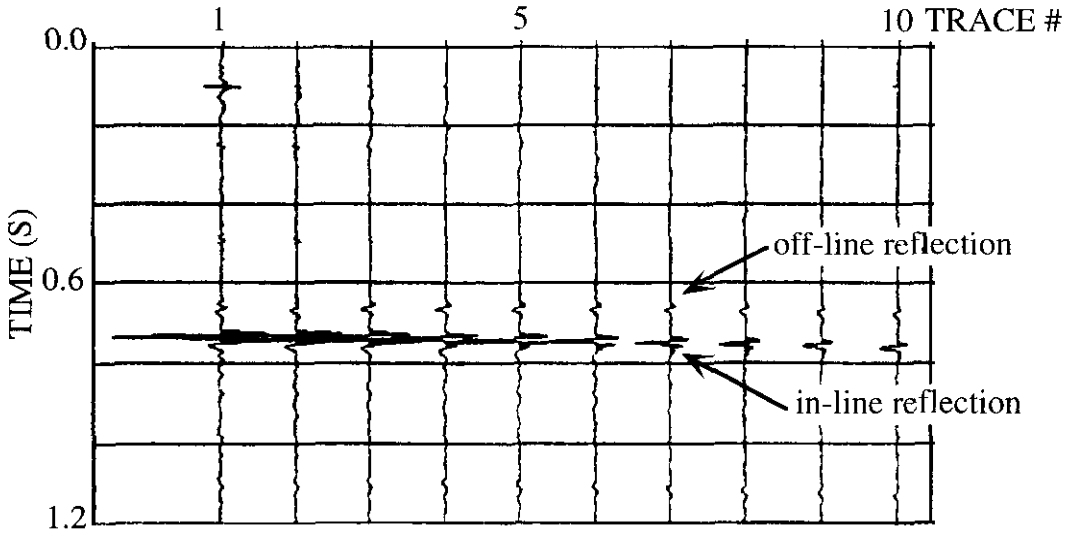

(a) vertical component.

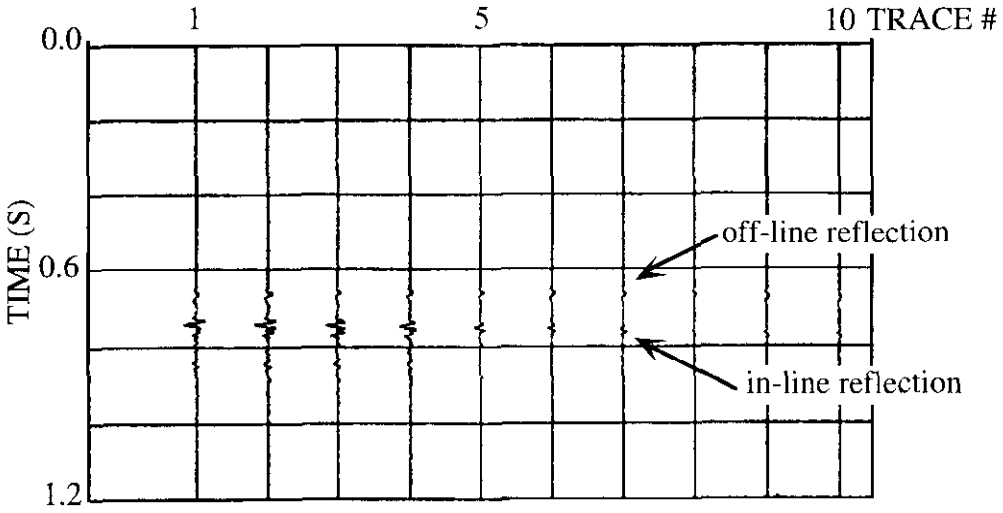

(b) transverse component.

Fig. 5. A shot record of physical modeling data.

and build an off-line image. The polarization filter can be applied on the raw data, if the data have a reasonably high S/N ratio to separate the in-line and off-line energy. Then we can use the filtered in-line data to create a better stacked section and the filtered off-line data to build an off-line image using conventional processing flow. If the data have low S/N ratio, an alternative way is to process the vertical and transverse components separately using conventional processing techniques (but not altering their relative amplitude), then to apply the polarization filter to the stacked sections of the vertical and transverse components to enhance the in-line image and build an off-line image. Because stacking does not change the polarization direction of the seismic data, we should still be able to obtain the correct polarization direction.

Conclusions

The direct least-squares (DLS) method is used to build a polarization filter. This filter was applied to a physical modeling data set. We successfully removed the off-line energy for a better in-line picture and built an off-line image. Polarization filtering can be used to detect and separate seismic waves from different directions. If we have three-component seismic data, we can use the polarization filter to: 1) attenuate the in-line energy and extract the off-line energy to build an off-line image; 2) attenuate the off-line energy to enhance the signal-to-noise (S/N) ratio of the conventionally processed sections. If the data have a low signal-to-noise ratio, some techniques like CMP stacking should be used to enhance signal before polarization filtering.

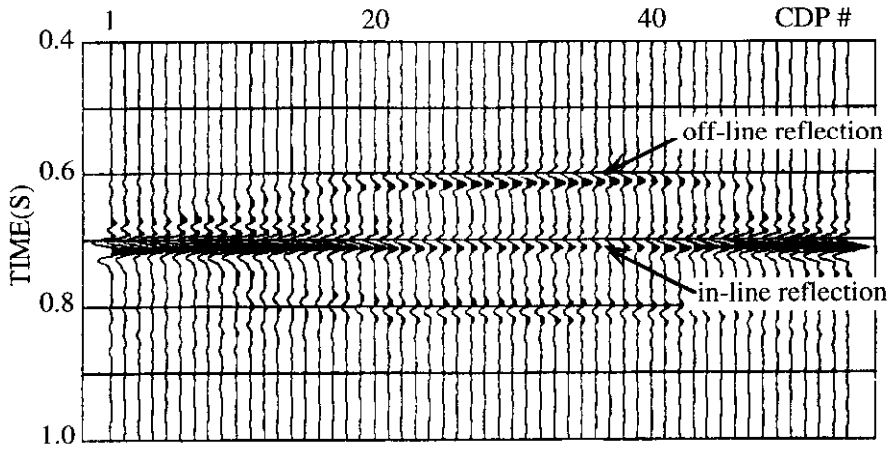

(a) vertical component.

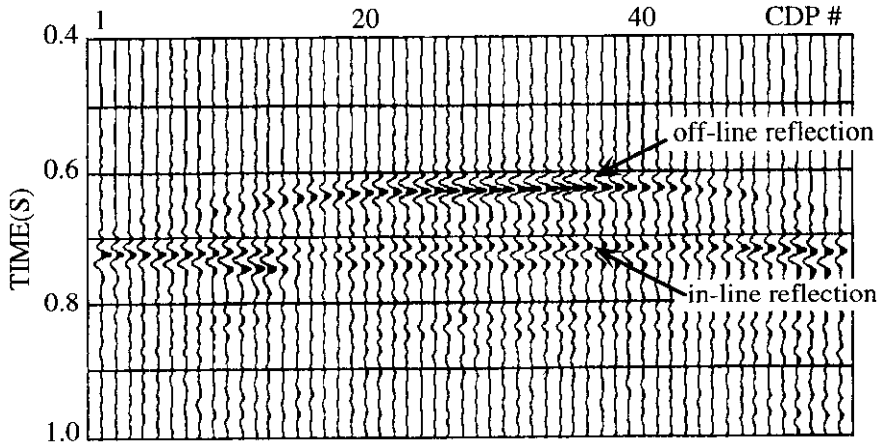

(b) transverse component.

Fig. 6. Conventional stacked sections of the physical modeling data.

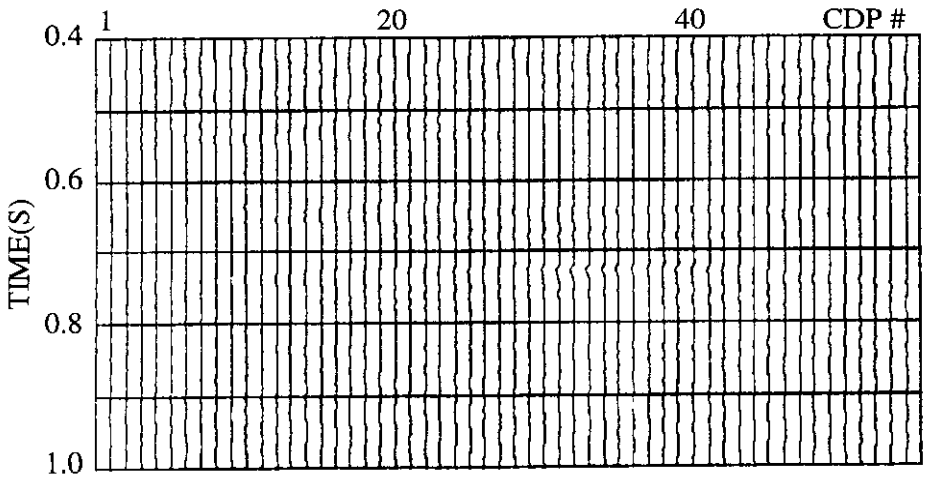

Fig. 7. Polarization filtered stack (50° - 85°). There is little coherent signal on the stack.

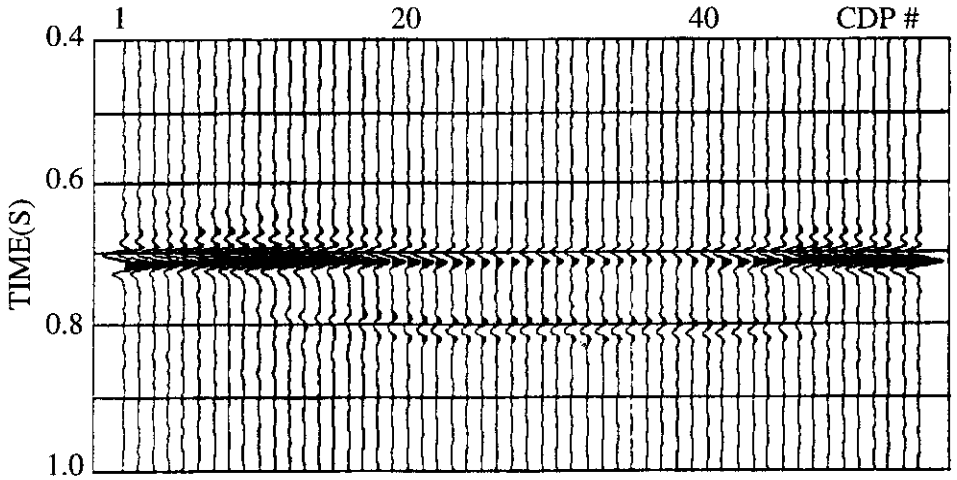

Fig. 8. Polarization filtered stack (85° - 93°). The image of the flat layer is on the stack and the off-line "reef" is removed. The event at the time 0.8 s is the reflection from point A in Figure 3.

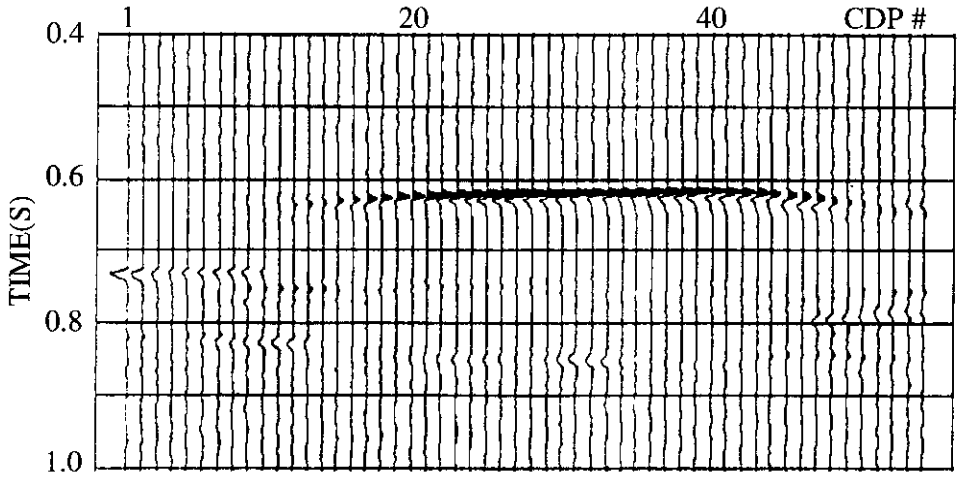

Fig. 9. The polarization filtered stack (95° - 105°). This is an off-line image. Most of the in-line reflection is removed.

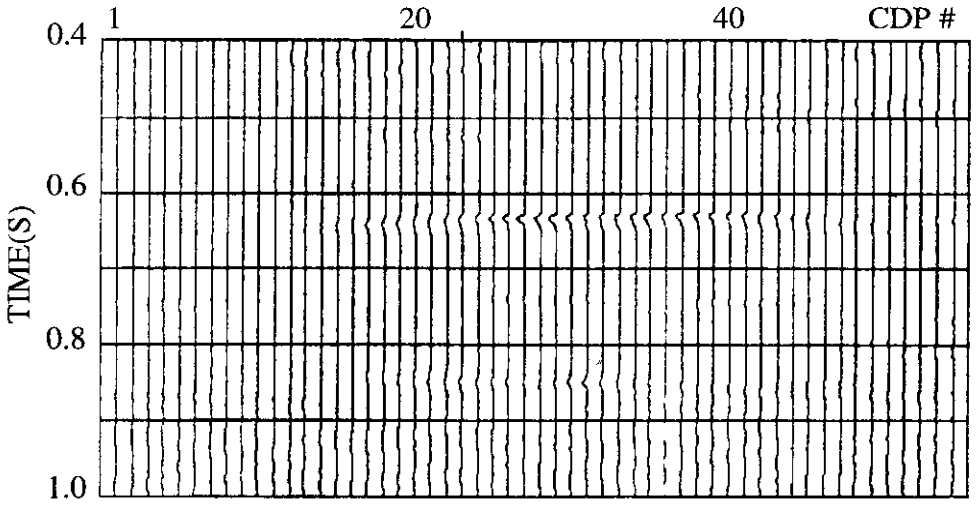

Fig. 10. The polarization filtered stack (105° - 150°). There is some "reef" energy on the stack but most energy from directly beneath the line has been removed.

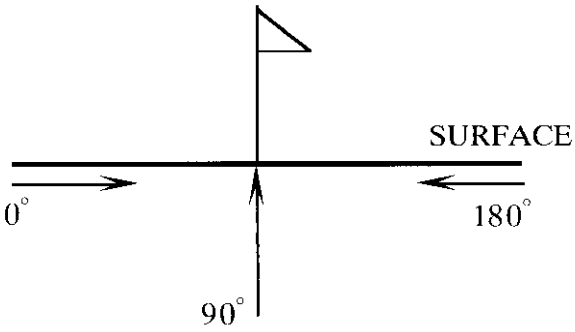

Fig. 11. Definition of direction.

ACKNOWLEDGMENT

The authors thank all staff of the CREWES Project of The University of Calgary for computer software, hardware support and physical modeling experiment. Thanks also to the sponsors of the CREWES Project for providing much appreciated financial support.

REFERENCES

Bataille, K. and Chiu, J.M., 1991, Polarization analysis of high-frequency, three-component seismic data: Bull. Seis. Soc. Am., **81**, 622 - 642.

DiSiena, J.P., Gaiser, J.E., and Corrigan, D., 1984, Horizontal components and shear wave analysis of three-component VSP data: In Toksoz, M.N. and Stewart, R.R., Eds., Vertical Seismic Profiling, Part B: Advanced Concepts: Geophysical Press.

Flinn, E.A., 1965, Signal analysis using rectilinearity and direction of particle motion: Proc. I.E.E.E., **53**, 1874 - 1876.

Kanasewich, E.R., 1981, Time sequence analysis in geophysics: The University of Alberta Press.

Montalbetti, J.F., and Kanasewich, E.R., 1970, Enhancement of teleseismic body phases with a polarization filter: Geophys. J.R. Astro. Soc., **21**, 119 - 129.

Perelberg, A.I. and Hornbostel, S.C., 1994, Applications of seismic polarization analysis: Geophysics, **59**, 119 - 130.

Zheng, Y., 1995, Seismic polarization filtering: noise attenuation and off-line imaging: M.Sc. thesis, Univ. of Calgary.

_____ and Stewart, R.R., 1993, Polarization filtering of three-component seismic data: Presented at the 1993 Ann. Nat. Mtg., Can. Soc. Expl. Geophys., Calgary, Canada.

_____ and Stewart, R.R., 1994, Off line imaging using 3-component seismic data: 64th Ann. Internat. Mtg., Soc. Expl. Geophys., Expanded Abstracts, 1442 1444.